Nonlinear electroreflectance from gallium nitride using optical second-harmonic generation

J. Miragliotta* and D. K. Wickenden
The Johns Hopkins University, Applied Physics Laboratory, Johns Hopkins Road, Laurel, Maryland, 20723-6099
(Received 5 July 1995)

The nonlinear optical properties of an electrified GaN film in contact with an electrolytic solution were investigated using second-harmonic (SH) generation. For SH photon energies near the fundamental absorption edge, a strong two-photon resonance was observed in the reflected SH signal when a surface dc electric field in the range of 110–575 kV/cm was applied to the GaN/electrolyte interface. The resonance was attributed to electric-field-induced SH (EFISH) generation, a third-order nonlinear response that generates a signal intensity that is quadradically dependent on the dc field in the film. The width of the EFISH resonance at the E_0 critical point was much narrower than the dispersion of the intrinsic $\chi^{(2)}$ nonlinearity but comparable to the linear electroreflectance response ($\omega_{in}=\omega_{out}$) in the band-edge region. The nonlinear results from GaN demonstrate the potential of the 2ω response for spectroscopic examination of critical points in the band structure of semiconductors. In addition to the spectral analysis, a fixed-frequency EFISH measurement at the peak of the resonance (3.43 eV) determined the magnitude of the third-order nonlinearity, $\chi^{(3)}_{zyyz}(-2\omega;\omega,\omega,0)$, to be 5.3×10^{-19} m^2/V^2.

I. INTRODUCTION

The ability of an applied dc field to perturb the optical properties of semiconductors has been the underlying basis of many forms of optical spectroscopy since the discovery of the electroreflectance (ER) effect nearly 30 years ago.[1] Considerable amounts of information regarding the electronic band structure of semiconductors can be obtained from these analytical techniques since field-induced perturbations are resonantly enhanced near critical point energies in the joint density of states (JDOS).[2,3] Although the dielectric variations $\Delta\varepsilon(\omega)$ are generally on the order 10^{-3} of the unperturbed function, modulation procedures have little difficulty observing their subsequent effect on the linear ($\omega_{in}=\omega_{out}$) reflective or absorptive properties of the illuminated material.[4,5]

An aspect of linear ER that has been recognized since the work of Aspnes in the early 1970s is the ability to treat the induced effect as a third-order nonlinear phenomena provided the applied dc field is sufficiently weak.[6–8] As a third-order response, the process involves the coupling of two dc fields and one optical field with the third-order susceptibility, $\chi^{(3)}(-\omega;\omega,0,0)$. This mixing process induces a nonlinear electric polarization at the same frequency of the incident optical source which generates a variation in the linear dielectric function, $\varepsilon(\omega)$. Another dc-field-dependent third-order nonlinear phenomena that occurs in semiconductors is electric-field-induced second-harmonic (EFISH) generation.[9–11] This nonlinear process couples two optical fields of frequency ω with one dc field so as to generate a second-harmonic (SH) polarization that is linearly dependent on the applied dc field. Unlike second-order SH,[12] the EFISH response arises from a third-order susceptibility $\chi^{(3)}(-2,\omega,\omega,\omega,0)$, which permits the generation of 2ω radiation in either centrosymmetric or noncentrosymmetric media. The EFISH susceptibility is similar to $\chi^{(3)}(-\omega;\omega,0,0)$ since it can be enhanced near electronic transitions such as critical point resonances in the JDOS of semiconductors. In fact, EFISH has been used as a spectroscopic probe in many organic systems,[13,14] and has recently proved useful in the analysis of one-dimensional excitons in thin films of linear-Si-chain compounds.[15] Also, the dispersive nature of the dc-field-induced 2ω response has been theoretically examined for semiconductor quantum-well structures,[16–18] but previous experimental studies of bulk material have been limited to single-wavelength investigations.[9,19–22]

In this paper, we shall show that the EFISH response from a moderately doped, *n*-type GaN film is resonantly enhanced when the photon energy of the SH field is tuned through the direct fundamental absorption edge (E_0 critical point). Analogous to the ER effect at frequency ω, the dc-field-dependent signal at 2ω was spectrally localized at the E_0 critical point with a magnitude that exceeded the intrinsic second-order nonlinearity when a field on the order of 10^5 V/cm was applied to the GaN surface. The EFISH signal exhibited a quadratic dependence to the depletion-layer field in the range between the flatband value up to 490 kV/cm. This behavior has been observed in previous fixed-frequency SH measurements by Qi *et al.*[20] on *n*-type GaAs(001) in air and Lantz and Corn[21] on *n*-type TiO_2 in an aqueous solution. In the present investigation, the resonant nature of the EFISH response illustrated the ability of field-induced SH as a spectroscopic probe of critical points in semiconductors. In addition to the spectroscopic investigations, a fixed-frequency, variable dc-field analysis of the EFISH signal at the band edge determined a field-induced SH nonlinear susceptibility of 7.0×10^{-11} m/V at an applied dc field of 440 kV/cm, a value that is five times larger than the intrinsic value of $\chi^{(2)}$ in the bulk material.[23]

II. EXPERIMENT

The details regarding the metal-organic chemical-vapor deposition (MOCVD) of epitaxial GaN on sapphire have been previously discussed.[24] Briefly, thin film samples were grown in a vertical spinning-disc MOCVD reactor operating at a pressure of 70 Torr. Source materials for film growth were trimethyl gallium and ammonia with nitrogen as the carrier gas. Before initiating continuous film growth at 1050 °C, a GaN nucleation layer of ~450 Å was predeposited on a 600 °C substrate by exposing the surface to the source materials for 50 s. During epitaxial growth, the samples were doped with silicon (SiH_4) so as to yield carrier concentrations in the low 10^{17} to mid 10^{18} cm^{-3} range. The single-crystal film was oriented with the (00.1) surface parallel to the (00.1) surface of the substrate. In addition, a 30° azimuthal rotation of the GaN layer with respect to the underlying sapphire substrate was verified by x-ray diffraction.

A dc field was applied to the GaN sample by placing the semiconductor film in contact with a HCl aqueous solution. The dc potential difference and field strength in the GaN depletion layer were controlled with a standard potentiostat in a three-electrode quartz cell using a Pt counter electrode and a saturated calomel reference electrode (SGE). An indium solder, low-resistance Ohmic contact was made to the front surface of the GaN film and subsequently covered with an epoxy cement to prevent contamination of the cell solution. The surface area of the GaN electrode exposed to the electrolyte solution was approximately 0.1 cm^2. The sample was cleaned in a hot, sulfuric and nitric acid aqueous solution for 10 min, rinsed with singly distilled and deionized water, and placed in a 0.1*M* HCl solution. In performing ac current measurements, a 3-kHz, 10-mV rms ac voltage was superimposed on the dc applied potential. The ac component of the current was analyzed with a two-phase lock-in amplifier (EG&G 5206). In both dc and ac current measurements, the dc applied potential was swept at a rate of 50 mV/s between the anodic and cathodic limits. The relatively high conductivity in the solution phase and undepleted region of the semiconductor assured that potential drops in these respective regions were negligible when compared to the depleted region of the semiconductor.[25,26] As such, the potential drop across the depletion layer was equated to the applied potential difference between the indium contact on the semiconductor and the reference electrode in the solution.

The nanosecond pulse, tunable dye laser source used for the SH measurements, has been previously described in the literature.[27] *S*-polarized laser radiation was incident at an angle of 45° to the GaN/electrolyte interface so as to generate a specularly reflected *p*-polarized SH signal. Typical incident power densities at the GaN surface were kept below 1 MW/cm^2 so as to minimize sub-band-gap photocarrier generation from possible deep-level traps in the GaN sample.[28] Under these incident conditions, the SH conversion efficiency at the absorption band edge was observed to produce ~10^8–10^9 photons/pulse. At this fluence level, the resultant screening of the dc field in the depletion layer from photogenerated electron-hole pairs (assuming a 1:1 SH photon to photocarrier ratio) was determined to be minimal. The reflected intensity at 2ω was detected with a high-gain photomultiplier tube (PMT), analyzed with a gated integrator, and normalized to a SH spectrum from a nonlinear optical standard material (quartz). The harmonic nature of the sample signal was verified by demonstrating its quadratic dependence to the incident light intensity.

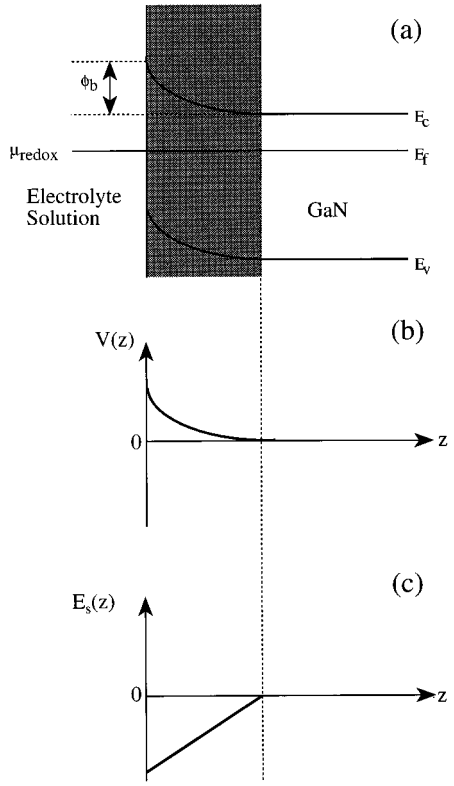

FIG. 1. (a) Equilibrium energy band diagram for an electrolyte/GaN interface. Upon contact, and electron transfer from the semiconductor to the solution equates the Fermi energy, E_f, of the GaN and the chemical potential of the solution, μ_{redox}. This creates a diffusion barrier, ϕ_b, and a depletion layer in the semiconductor (shaded region). (b) The electrostatic potential and (c) field as a function of distance into the depletion layer.

Differential reflectance measurements at ω were performed using a standard linear optical arrangement.[29–31] In these experiments, *p*-polarized light from a xenon lamp was transmitted through a monochromator and focused onto the GaN/electrolyte interface at an angle of 45°. The electric field in the depletion layer was modulated between the flatband (zero field) and a reverse bias condition by superimposing an ac square-wave voltage (220 Hz) on the dc potential. After detection with a PMT, the ac component of the reflected light was analyzed with the two-phase lock-in amplifier and normalized to the zero dc field reflectance.

III. ELECTROCHEMICAL RESULTS AND DISCUSSION

Characterization of the dc field in the GaN sample required a number of ac and dc electrochemical measurements prior to the SH reflectance studies. After placing the GaN in the solution in an open circuit configuration, equilibrium was established at the interface by an electron transfer from the *n*-type GaN to the electrolyte. As is shown in Fig. 1(a), the chemical potential of the acidic solution, defined as the

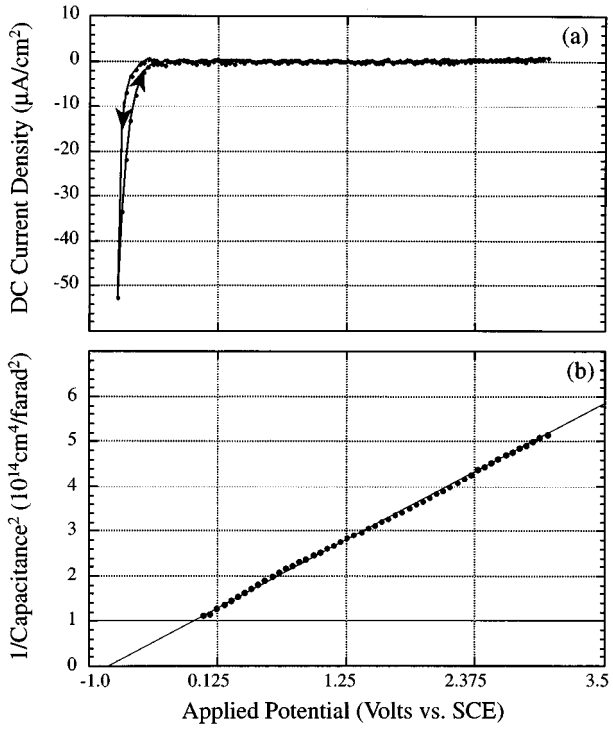

FIG. 2. (a) dc current versus applied potential scan of GaN in 0.1*M* HCl solution. Potentials positive of -0.75 V represent a reverse-biased GaN/electrolyte interface. At a potential that is negative of this value, H_2 evolution occurs. Arrows indicate the direction of the potential scan. (b) Mott-Schottky plot for a GaN epitaxial sample in 0.1*M* HCl aqueous solution. Solid line is a linear fit to the experimental data (solid circles).

H_2/H^+ redox potential, was equated with the Fermi energy in the semiconductor after the charge transfer.[32] Equilibrium at the interface resulted in a diffusion barrier (ϕ_b) and a depleted carrier region (shaded area) which was characterized by conduction- and valence-band bending. Employing the Schottky approximation to the charge density in the GaN depletion layer,[33] the dc potential and field in this space-charge region were assumed to exhibit a quadratic and linear decrease, respectively, with distance into the sample [see Figs. 1(b) and 1(c)].

Modulation of the band-bending, barrier height, and depletion-layer thickness was accomplished by varying the potential difference between the bulk regions of the solution and the GaN sample. This procedure shifted the position of the redox potential relative to the Fermi level so as to increase (reverse bias) or decrease (forward) the barrier height at the interface. Figure 2(a) shows the dc current density versus applied potential for the GaN/electrolyte interface as the applied potential was swept between -1.00 and $+2.75$ V. We note that in all measurements, the applied potential was defined as the potential of the GaN sample relative to the SCE reference electrode. At a potential negative of -0.75 V, defined as the flatband potential, a forward biased dc current was observed in the GaN sample which evolved H_2 at the GaN surface. At potentials positive of -0.75 V (reverse bias), the current density was below the detectable limits of our potentiostatic amplifier ($<0.01\ \mu A/cm^2$).

The dopant concentration and surface dc field were determined from a Mott-Schottky (MS) analysis of ac impedance measurements.[25,26,34] Figure 2(b) shows the MS data (solid circles), capacitance^{-2} versus applied potential, for the *n*-type GaN sample. In the evaluation, the electrolyte/semiconductor interface was modeled as an electrical circuit composed of a resistor (solution) and capacitor (depletion layer) in a series combination, a representation that has been used in previous electrochemical investigations.[26] Using the assumption of an ideal Schottky barrier at the liquid/solid junction, the equation for capacitance^{-2} of the depletion-layer region is[26,34]

$$C^{-2}=\frac{2}{q\varepsilon_0\varepsilon_s N_d}\left(V_{\text{bias}}-V_{\text{fb}}-\frac{kT}{q}\right), \tag{1}$$

where V_{bias} is the externally applied potential, V_{fb} is the flatband potential, N_d is the carrier concentration, ε_s is the static dielectric constant [GaN has a value of $\varepsilon_s=9$ (Ref. 48)], ε_0 is the dielectric permittivity constant, C is the space-charge capacitance per unit area, k is the Boltzmann constant, T is the temperature, and q is the electronic charge. The solution component of the interfacial capacitance (Helmholtz and Gouy capacitance) has been ignored in this analysis since it was two orders of magnitude larger than the corresponding value in the depletion layer. The series combination of the solution and semiconductor capacitance assured that the smaller of these two components would dictate the behavior of the total interfacial capacitance. The MS data was fitted to the expression in Eq. (1) (solid line) which determined a value of 3.0×10^{17} cm^{-3} and -0.79 V for N_d and V_{fb}, respectively, at room temperature. This latter value was in good agreement with the potential associated with the onset of a forward bias current [flatband potential ~-0.75 V, Fig. 2(a)]. No variation in the values of N_d and V_{fb} were observed in the *C-V* measurements for modulation frequencies up to 30 kHz.

The electrostatic field in the depleted layer was determined by solving Poisson's equation[35] and using the values of N_d and V_{fb} from the MS measurement

$$E_s(z)=\frac{qN_d}{\varepsilon_0\varepsilon_s}[z-z_0], \tag{2a}$$

where

$$z_d=\left\{\frac{2\varepsilon_0\varepsilon_s}{qN_d}\left[V_{\text{bias}}-V_{\text{fb}}-\frac{kT}{q}\right]\right\}^{1/2} \tag{2b}$$

In these two expressions, $E_s(z)$ is the electrostatic field, z is the distance into the GaN sample, and z_d is the depletion-layer thickness. For the SH measurements, the magnitude of the dc field at the surface ($z=0$) was determined to range between 110 and 576 kV/cm for the reverse bias potential range of $+0.1$ to $+2.75$ V (relative to the flatband value). In this same range of potentials, the width of the depletion layer was calculated to vary between 0.02 and 0.1 μm. In all SH measurements, the semiconductor was kept at a reverse bias potential in order to minimize hydrogen evolution at the GaN surface.

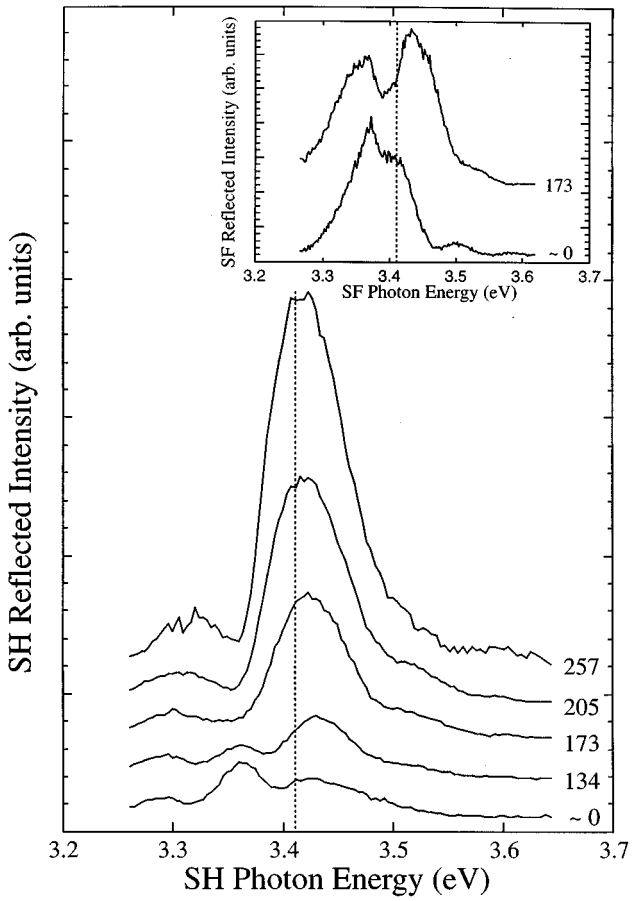

FIG. 3. Reflected SH intensity from an electrolyte/GaN interface as a function of the SH photon energy. The dashed line represents the position of the band edge in the unbiased sample. The number to the right of each spectrum is the value of the dc field at the GaN surface in kV/cm. The spectra in the inset shows the SF intensity from the same GaN sample recorded using a fixed 532-nm and tunable IR source (see text).

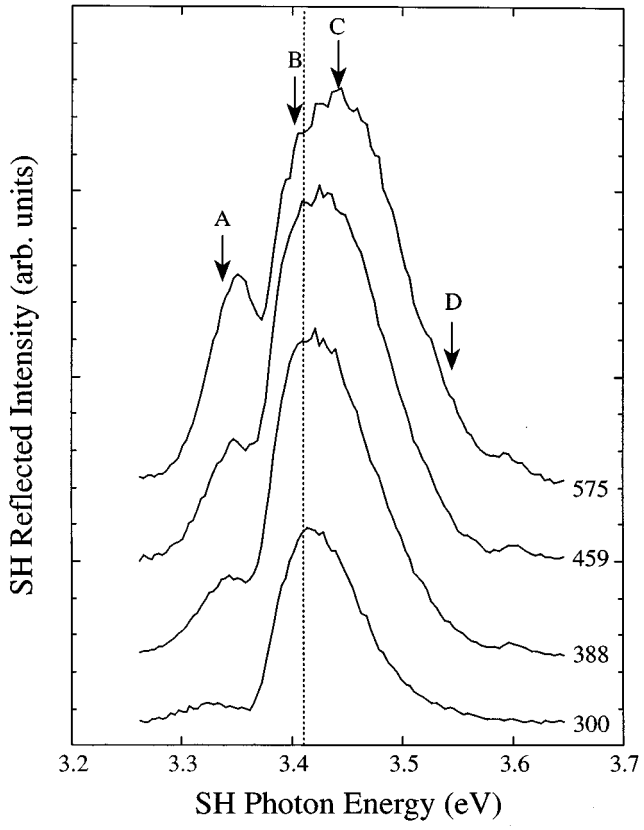

FIG. 4. Reflected SH intensity from an electrolyte/GaN interface as a function of the SH photon energy. The number to the right of each spectrum is the value of the dc field at the GaN surface in kV/cm. The positions A–D are the photon energies used for the variable dc-field measurements in Fig. 6.

IV. NONLINEAR ELECTROREFLECTANCE RESULTS

The spectra in Figs. 3 and 4 show the effects of the depletion-layer dc field on the SH reflected intensity from a GaN/electrolyte interface. The dashed vertical line in both graphs denotes the position of the fundamental absorption edge, $E_{\text{gap}} \sim 3.41$ eV, as determined from linear absorption measurements from the unbiased GaN sample. In the flat-band spectrum shown in Fig. 3 (0 V/cm), two weak peaks were observed at SH photon energies just below the band-edge position. The SH profile in this photon energy region was found to be dependent on film thickness and incident angle, a result that was attributed to the phase-velocity interference between the nonlinear source polarization and the generated SH field.[36] The zero-dc-field spectrum, dependent only on the intrinsic $\chi^{(2)}$ of the GaN, exhibited weak dispersion in the SH photon energy range above the band edge which was consistent with previous measurements of $\chi^{(2)}$ in wurtzite GaN.[23]

With the application of a reverse-bias dc field, significant changes were observed in both the magnitude and dispersion of the SH response. At an applied potential of $+0.15$ V relative to the flatband value, corresponding to a surface dc field of 134 kV/cm, the EFISH contribution was characterized by a single resonance at 3.43 eV with a linewidth value of ~ 50 meV. The resonance increased monotonically in amplitude as the surface field was increased to 257 kV/cm with a slight decrease in energy position (3.41 eV) and a broadening in the linewidth. Below the band edge, a significant change in the spectral profile was manifested by a reduction in the number of interference peaks from two to one as the surface field was increased to 173 kV/cm. The field-dependent behavior shown in Fig. 3 was observed in all n-type GaN samples regardless of doping concentration (0.1–3.0×10^{18} cm^{-3}), incident optical polarization and angle, and incident power density.

As a complementary measurement to the SH response, a sum-frequency (SF) measurement was performed to determine whether the resonance in the EFISH spectra was due to a one-photon interaction with mid-gap states or a 2ω resonance with the band-edge critical point. In this experiment, a SF signal with a photon energy in the band-edge region was generated via coherent mixing of an incident tunable IR laser source (0.93–1.32 eV) and a fixed visible laser source at 2.34 eV. The photon energy of each beam was sufficiently shifted from the incident beam used in the SH measurements which eliminated the possibility of coincidental, one-photon resonances with mid-gap states. As is shown in the inset of Fig. 3, the SF spectrum recorded with surface field of 173 kV/cm

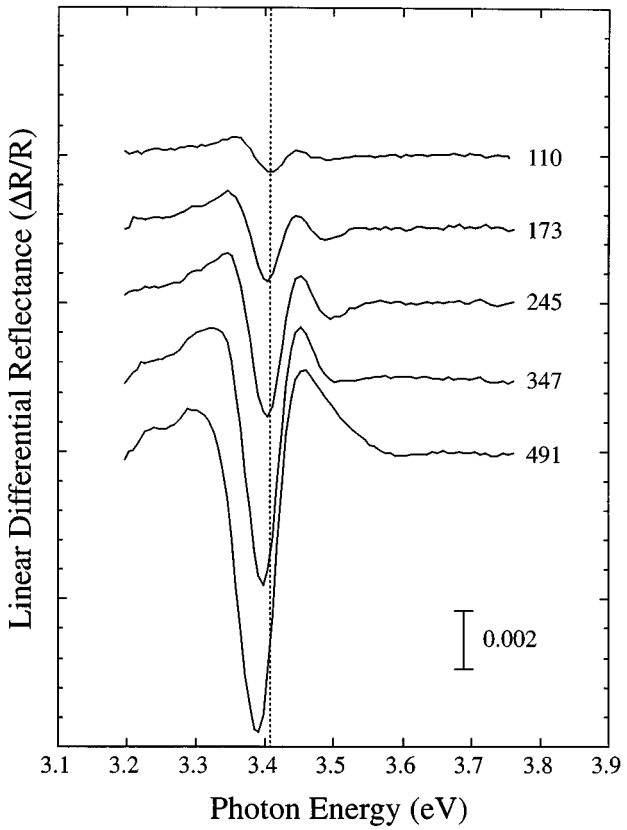

FIG. 5. Linear differential reflectance spectra from an electrolyte/GaN interface as a function of the incident photon energy. The dashed line represents the position of the band edge in the unbiased sample. The number to the right of each spectrum is the value of the field at the GaN surface (kV/cm) during the reverse-bias portion of the square-wave modulated potential (220 Hz).

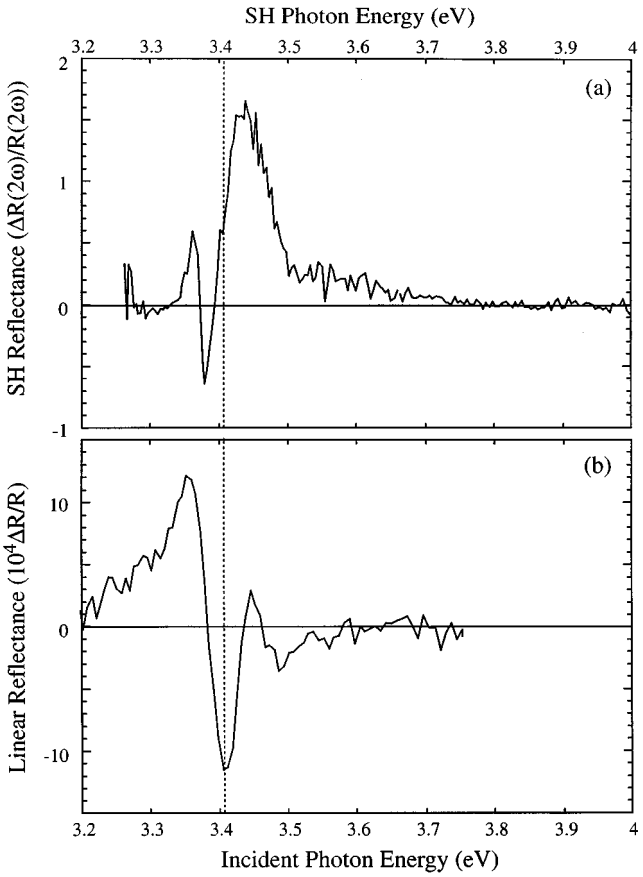

FIG. 6. (a) Differential SH reflectance and (b) differential linear reflectance from a GaN/electrolyte interface recorded under a surface field modulation of 0–110 kV/cm. In (a), the spectrum was measured as a function of the SH photon energy at a field modulation rate of 5 Hz. In (b) the scan was measured as a function of the incident photon energy at a modulation rate of 220 Hz.

showed a resonant peak at the same energy as was observed in the SH results, confirming the two-photon nature of the EFISH resonance.

The spectra in Fig. 4 showed that the resonant peak amplitude continued to increase as the surface dc field was increased to 575 kV/cm. Considerable broadening was observed in the 388–575-kV/cm spectra as shown by the extension of SH enhancement to photon energies well above (>0.2 eV) and below (~ 0.1 eV) the band-edge position. In the 575-kV/cm scan, the degree of linewidth broadening below the band-edge energy led to an apparent splitting in the resonance near 3.38 eV. Although the proximity to the band-edge energy makes an accurate determination of the linewidth very difficult, the resonant profile in this spectrum was clearly greater than 0.2 eV.

In addition to the SH measurements, Fig. 5 shows the differential linear ER spectra ($\omega_{\text{in}} = \omega_{\text{out}}$) recorded at the E_0 critical point for a range of applied dc fields that coincided with a number of SH scans in Figs. 3 and 4. Similar to the EFISH response, the negative peak associated with the E_0 optical resonance broadened in linewidth and shifted to lower energies as the applied dc field was increased in the GaN depletion layer. The amplitude of the E_0 resonance increased linearly with the applied potential which was consistent with previous linear ER results from moderately doped III-V semiconductors in an electrochemical environment.[29,30] Also, Franz-Keldysh oscillations (FKO) appeared at photon energies above the band edge (dashed line), with a period that increased with increasing dc field. As a comparison to the linear differential measurements in Fig. 5, a differential measurement of the SH reflectance was also performed on the GaN sample. In this measurement, the applied bias to the GaN sample was modulated at a repetition rate of 5 Hz so as to vary the surface dc field from the flatband value to 110 kV/cm. The dc-field modulation and laser repetition were temporally synchronized so that sample illumination occurred during the flatband and the reverse-bias conditions. At the end of each potential cycle, the difference between the reverse-bias and flatband signals was normalized to the flatband response. The results from a typical differential scan are shown in Fig. 6(a). In this plot, the spectral range was extended to 4 eV so as to monitor the EFISH contribution well above the band-edge position. Each data point in the spectrum represented the average SH differential value after 10 applied potential cycles. At SH energies above the band-edge position (vertical dashed line), the differential signal was characterized by a positive-valued peak located at 3.43 eV which was consistent with the location and linewidth of the EFISH resonance in the Fig. 3 spectra. The peak amplitude exceeded the flatband intensity by a factor of 1.5 and

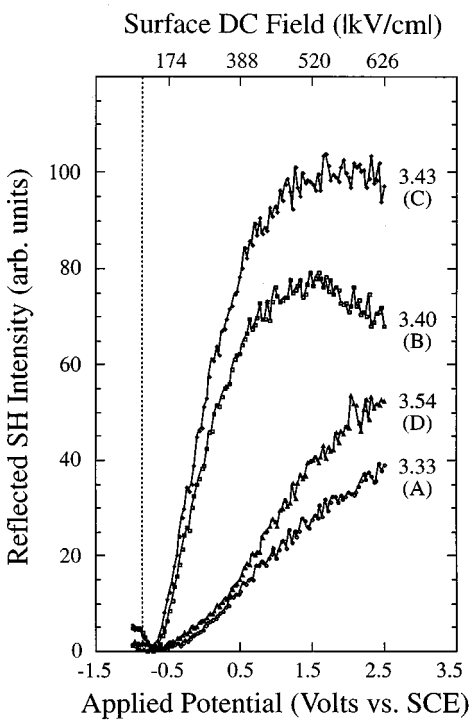

FIG. 7. A series of fixed-frequency SH reflectance scans from a GaN/electrolyte interface as a function of the applied potential. The SH photon energy of each scan (A–D) is given at the right of each scan in eV.

monotonically decreased to zero as the SH photon energy was tuned to 3.8 eV. Repeated differential measurements in the spectral region above the band-edge region on a series of GaN samples showed that the SH response was unaffected by film thickness, doping, or incident angle. However, the oscillation in the signal profile below the band edge was found to be dependent on the optical path length in the sample. Due to the high transmissivity of the GaN film in this wavelength range, this behavior was attributed to the aforementioned phase-velocity mismatch interference effect. In addition to the SH scan, the 110 kV/cm result from the linear $\Delta R/R$ scan is shown in Fig. 6(b).

The spectra in Figs. 3 and 4 indicated that the applied potential dependence of the EFISH effect at photon energies either "on" or "off" the initial resonant peak position would display markedly different behaviors. As a check of this hypothesis, a series of fixed photon energy, variable surface dc-field scans was measured over a range of energies that encompassed the profile of the EFISH resonance (positions A–D in Fig. 4). The results of this procedure are shown in Fig. 7. For all SH energies in the band-edge region, the SH signal exhibited a decrease relative to the intrinsic $\chi^{(2)}$ nonlinearity as the applied potential was tuned just positive of the flatband potential (dashed vertical line). In the "on" resonance scans (B and C), a minimum in the signal intensity was observed at $+0.1$ V (relative to the flatband) followed by a rapid increase in the 174–388-kV/cm region. Above these surface field strengths, the signal level began to saturate at both SH energies with a 12% decrease in scan B for field amplitudes above 520 kV/cm. In scans A and D (below and above the peak position, respectively), the initial decrease in the SH signal reached a minimum by $\sim+0.25$ V above the flatband potential with a subsequent rate increase that was one-third that observed in scans B and C. At these two energies, signal saturation was not observed in the high-field region, but the intensity remained well below the peak levels observed in the "on" resonance scans.

V. THEORY AND DISCUSSION

In the case of GaN, the 2ω polarization response from an electrified sample is a linear combination of an intrinsic second- and dc-field-dependent third-order nonlinear contribution. In the present experimental arrangement, the dc field was directed along the optical axis of the GaN sample (perpendicular to the semiconductor surface) which corresponded to the z axis in both the crystal and laboratory coordinate frame of reference. The xy plane of the crystal (surface plane) was rotated about the optical axis until the plane of incidence coincided with the xz plane of the crystal. For the wurtzite phase of GaN ($6mm$ symmetry), the independent components of $\chi^{(2)}$ and $\chi^{(3)}$ that can contribute to the SH response for an arbitrary incident polarization and a dc field directed along the optical axis are $\chi^{(2)}_{zyy}$, $\chi^{(2)}_{yzy}$, $\chi^{(2)}_{zzz}$, and $\chi^{(3)}_{zyyz}$, $\chi^{(3)}_{yzyz}$, $\chi^{(3)}_{zzzz}$, respectively.[37] When using an incident light source that is s polarized (along the y axis of the crystal), the nonlinear polarization from the electrified GaN sample is induced along the optical axis (p polarized) and contains a single $\chi^{(2)}$ and $\chi^{(3)}$ tensor element:

$$P_z^{\mathrm{ln}}(z,2\omega)=\chi_{\mathrm{eff}}^{\mathrm{nl}}(z)E_y^2(z,\omega), \tag{3a}$$

where the effective nonlinearity $\chi_{\mathrm{eff}}^{\mathrm{nl}}(z)$ is given by[37]

$$\chi_{\mathrm{eff}}^{\mathrm{nl}}(z)=\chi^{(2)}_{zyy}(-2\omega;\omega,\omega)+3\chi^{(3)}_{zyyz}(-2\omega;\omega,\omega,0)E_s(z). \tag{3b}$$

In these two expressions, $E_y(z,\omega)$ is the y component of the fundamental field and $E_s(z)$ is the dc field directed along the optical axis [Eq. (2a)].

The reflected SH intensity from the GaN sample is dependent upon the product of the nonlinear polarization and its conjugate:[38]

$$I_{\mathrm{SH}}\rightarrow P_z^{\mathrm{nl}}(z,2\omega)^*P_z^{\mathrm{nl}}(z,2\omega). \tag{4a}$$

$$=\chi^{(2)}_{zyy}|^2+|3\chi^{(3)}_{zyyz}E_s(z)|+6E_s(z)|\chi^{(3)}_{zyyz}\chi^{(2)}_{zyy}|\cos\psi, \tag{4b}$$

where the wavelength notation on the field and susceptibilities have been omitted for simplicity. The reducing or enhancing nature of the EFISH contribution will depend on the relative phase difference between the second- and third-order susceptibilities (ψ) and the sign of the dc field in the depletion layer. The z dependence of the dc field must also be considered in calculating the reflected intensity at 2ω, which is shown in the Appendix.

In addition to the relative phase and dc-field dependence, the spectral linewidth of the SH response in the band-edge region is dependent on the dispersion of both second- and third-order susceptibilities. A comparison of the flatband SH spectrum with the EFISH response in Figs. 3 and 4 show that the dispersion of $\chi^{(3)}_{zyyz}(-2\omega;\omega,\omega,0)$ is markedly narrower than the corresponding response of $\chi^{(2)}_{zyy}(-2\omega;\omega,\omega)$ in the

band-edge region. Recently, full band-structure calculations of $\chi^{(2)}(-2\omega;\omega,\omega)$ have been performed on a number of bulk cubic zinc-blende III-V and II-VI semiconductors over a range of photon energies that include the E_0 critical point in the JDOS.[39–42] In the second-order nonlinearity, which is proportional to the product of three dipole-matrix elements, Ghahramani *et al.* have shown that the various transitions between valence and conduction bands in the semiconductor band structure lead to either virtual-electron or virtual-hole contributions to $\chi^{(2)}(-2\omega;\omega,\omega)$.[40,41] However, in II-VI and III-V materials such as ZnSe and GaAs, the electron contribution to $\chi^{(2)}(-2\omega;\omega,\omega)$ has been shown to produce a positive-valued $\chi^{(2)}(-2\omega;\omega,\omega)$ for 2ω photon energies below the band edge with a magnitude that is significantly larger than the corresponding virtual-hole transitions. Under conditions where the 2ω photon energy is near the resonance with the fundamental band edge, the second-order susceptibility is proportional to

$$\chi^{(2)}_{zyy} \propto \frac{\langle \psi^v_l|z|\psi^c_n\rangle\langle \psi^c_n|y|\psi^c_m\rangle\langle \psi^c_m|y|\psi^v_l\rangle}{(\omega_{\rm nl}-2\omega-i\gamma_{\rm nl})(\omega_{\rm ml}-\omega-i\gamma_{\rm ml})}, \tag{5}$$

where ψ^v_i and ψ^c_j are the wave functions for the ith and jth valence and conduction band, respectively. Also ω_{ij} is the energy separation and γ_{ij} is the broadening parameter for the i-to-j transition. In this expression, the summation over the valence band index l, and the conduction band indices n and m is implied. As is evident from this expression, the second-order nonlinearity is resonantly enhanced when either ω or 2ω is the frequency difference between two single-particle states (valence or conduction bands). In the present investigations, the SH experiments on GaN were performed with $2\hbar\omega \sim E_{\rm gap}$, which should generate a single resonance in the band-edge region since higher interband transition (E_1 critical point) are at least 4 eV above the fundamental gap.[43]

To the best of our knowledge, no calculations have been made pertaining to the EFISH susceptibility $\chi^{(3)}(-2\omega;\omega,\omega,0)$ in bulk, direct-gap semiconductors. A number of recent calculations by Tsang *et al.*[16–18] on the EFISH effect in semiconductor quantum wells have predicted a significant field-induced enhancement in the SH nonlinearity of GaAs/Al_xGaAs_{1-x} structures. In general, $\chi^{(3)}(-2\omega;\omega,\omega,0)$ is proportional to the product of four dipole-matrix elements and is similar to $\chi^{(2)}(-2\omega;\omega,\omega)$ in that it contains contributions from both virtual-electron and -hole transitions between the various valence and conduction bands in the band structure. In addition to the virtual transitions, the third-order susceptibility contains a contribution from ''three-state'' processes which involve simultaneous interband transitions between the valence and conduction bands.[40,44] The dipole-matrix elements for this term have been shown to be significantly larger than the virtual contributions in materials such as Si, GaAs, and ZnSe. Assuming that the three-state process is indeed the dominant contribution to $\chi^{(3)}_{zyyz}$, this expression is proportional to

$$\chi^{(3)}_{zyyz} \propto \frac{\langle \psi^v_l|z|\psi^c_\nu\rangle\langle \psi^c_\nu|y|\psi^v_n\rangle\langle \psi^v_n|y|\psi^c_m\rangle\langle \psi^c_m|z|\psi^v_l\rangle}{(\omega_{\nu l}-2\omega-i\gamma_{\nu l})(\omega_{\rm nl}-2\omega-i\gamma_{\rm nl})(\omega_{\rm ml}-\omega-i\gamma_{\rm ml})}, \tag{6}$$

when the 2ω photon energy is close to a resonance in the GaN band structure. The parameters in Eq. (6) are similarly defined as for Eq. (5). The form of Eq. (6) shows that the 2ω resonance in the EFISH signal is inversely proportional to the square of $(E_{2\omega}-E_{\rm gap})$ when SH photon energy is near the band edge ($\omega_{\nu 1}=\omega_{\rm nl}\sim\omega_{\rm gap}$). A qualitative comparison of Eqs. (5) and (6) shows that the third-order nonlinearity should have a narrower dispersion near the fundamental band edge provided the resonance is well-removed (minimal overlap) from other critical point transitions. The narrow resonance in the EFISH spectra in Fig. 3 supports this conclusion since the third-order nonlinear response was localized within $\sim\pm 0.1$ eV of the E_0 critical point while the intrinsic second-order nonlinearity (flatband spectrum) was significantly broader.

A comparison of the differential ER spectra at 2ω and ω (Fig. 6) show that the field-induced response in each respective case was spectrally localized at the E_0 critical point energy with different line-shape profiles. In the ω reflectance results, the magnitude of the dc-field-dependent perturbation energy[8]

$$h\Omega = \left[\frac{e^2E_s^2h^2}{8\mu}\right]^{1/3}, \tag{7}$$

where μ is the effective mass of electrons in GaN taken to be $0.22m_0$ (Ref. 49) and E_s is the dc field at the surface of the semiconductor. For the range of applied potentials used in this study, the value of this energy parameter ranged from 17 to 51 meV which was comparable to or greater than the broadening parameter for the E_0 critical point ($\sim$10 meV). The magnitude of this energy parameter negated the use of the Aspnes ''low-field,'' third-order nonlinear limit of linear ER (Refs. 6–8) and instead placed the dc field in the ''intermediate'' range of applied perturbations. The broadening and position shifts in the resonant peak as well as the FKO above the band edge were consistent with the intermediate field approximation as well as previous linear ER measurements on n-type GaAs samples with dopant concentrations in the 10^{17}–10^{18} cm^{-3} range.[30] In the 2ω case, broadening and peak shifts were also observed in the EFISH signal with increasing dc field, but the FKO were not observed at SH photon energies above the band edge. Another significant difference was the magnitude of the respective ω and 2ω field-induced effect relative to the zero-dc-field response. In the 2ω results, the EFISH contribution exceeded the intrinsic second-order response by over 100% with surface dc fields on the order of 10^5 V/cm while the same field strength produced ΔR values on the order of 10^{-3}. In an attempt to quantify the effects of the dielectric variations on the SH signal, the linear ER data in Fig. 5 was analyzed with the electromagnetic approach developed by Batchelor *et al.* in modeling the differential reflectance from n- and p-type GaAs in an electrochemical environment.[29] An expression for $\Delta R(\omega)/R(\omega)$ was derived for the GaN/electrolyte system that provided a determination of $\Delta\varepsilon(\omega)$ in each spectrum in Fig. 6. This analysis obtained values of $\Delta\varepsilon(\omega)$ on the order of 10^{-2} relative to the unperturbed $\varepsilon(\omega)$ when the dc field was 5.0×10^5 V/cm. The spectral behavior of the dielectric variation was substituted into a similarly derived expression for the SH reflection from the GaN sample (see

the Appendix) and calculated to produce variations in the 2ω signal that were 3–4 orders of magnitude *below* the $>100\%$ increase observed in the spectra of Figs. 3 and 4. This result confirmed that the narrow resonance in the SH spectra was clearly dominated by the behavior of the $\chi^{(3)}$ with little contribution from the field-induced dielectric variations that are characteristic of linear ER spectra. However, the similarities regarding the field-dependent broadening and peak shifts in the ω and 2ω suggest that the EFISH susceptibility has comparable sensitivity to critical point resonances in the band structure.

Examination of Eq. (3b) and the applied potential behavior of the fixed-frequency EFISH results in Fig. 7 indicated that the sign of $\chi^{(2)}_{zyy}(-2\omega;\omega,\omega)$ and $\chi^{(3)}_{zyyz}(-2\omega;\omega,\omega,0)$ must be the same since the application of a negative dc field [Eq. (2a)] produced an initial decrease in the SH signal. The position of the SH minima in the applied potential scans of Fig. 7 corresponded to the dc field at which the second- and third-order polarization terms in Eq. (3b) were equal. The SH response at the ''on'' resonance positions reached a minimum at a much lower applied field than was observed in the ''off'' resonance scans, which indicated that the ratio of the third-order to second-order susceptibility was higher near the EFISH peak position. The results in Fig. 7 were also to be used to determine the magnitude of the $\chi^{(3)}_{zyyz}(-2\omega;\omega,\omega,0)$ in the band-edge region. Quantitatively, the expressions in Eqs. (3) and (4) show that an evaluation of the third-order susceptibility required values of the dc field and $\chi^{(2)}_{zyy}(-2\omega;\omega,\omega)$ prior to the EFISH analysis. The former parameter was evaluated from the previously mentioned electrochemical studies while the latter term had been determined from the band-edge SH transmission measurements of GaN.[23] In the previous SH measurement, a value of 1.3×10^{-11} m/V was determined for $\chi^{(2)}_{zyy}(-2\omega;\omega,\omega)$ at a 2ω photon energy of 3.43 eV, which corresponds to the SH energy in scan *C* of Fig. 7. In modeling the field-dependent response, the data in this EFISH measurement was terminated at a surface dc field of 388 kV/cm [-0.5 V (SCE)] so as to avoid the potential region where broadening and shifting of the resonant peak was observed. As shown by the inset of Fig. 8, the electrified sample was treated as a depleted region with a characteristic depth denoted by z_d. The total nonlinear polarization in the depletion layer was given by the expression in Eq. (3a) while outside this region the polarization depended only on the intrinsic second-order susceptibility $\chi^{(2)}_{zyy}(-2\omega;\omega,\omega)$. Multiple reflections at 2ω in the film were ignored since the absorption coefficient in the GaN sample at this energy is $\sim6\times10^5$ cm^{-1} (Refs. 43 and 45) with an attenuation length of 0.033 μm. The value of depletion layer was calculated to exceed the attenuation length when the applied potential was greater than $+0.33$ V (SCE). The fitting procedure treated both $\chi^{(2)}$ and $\chi^{(3)}$ as real quantities while incorporating a phase difference (ψ) in the linear dc-field-dependent term of Eq. (4b). To approximate the effects of the linear variation of the dc field versus distance into the depletion layer *and* generate tractable analytical expressions for the reflection coefficient, the depletion layer was divided into a discrete number of slices (N) each of which contained a constant dc field. Applying the appropriate boundary conditions to Maxwell's equations at each nonlinear interface in the multilayer film, the reflection coefficient for the N-slice composite was derived. A complete description of the electromagnetic model with an expression for the reflection coefficient is given in the Appendix. The 2ω reflection data was fit to the reflection coefficient, given by Eq. (A2) in the Appendix, using a nonlinear least-squares routine with the only adjustable parameters in the model being the magnitude of the third-order susceptibility and the relative phase difference. The results of this fitting procedure are denoted by the solid lines in the data of Fig. 7. In obtaining the fit to data, a value of 5.3×10^{-19} m^2/V^2 was determined for $\chi^{(3)}_{zyyz}(-2\omega;\omega,\omega,0)$ with a relative phase difference of 0.55 rad. The magnitude of this value was consistent with a recent measurement of $\chi^{(3)}_{xxxx}(-3\omega;\omega,\omega,\omega)$ in GaN,[27] which determined a value of 3.8×10^{-19} m^2/V^2 at the band edge. For a surface field of 327 kV/cm, Eq. (3b) determined that the effective second-order nonlinearity at the GaN surface exceeded $\chi^{(2)}_{zyy}(-2\omega;\omega,\omega)$ by a factor of 5.

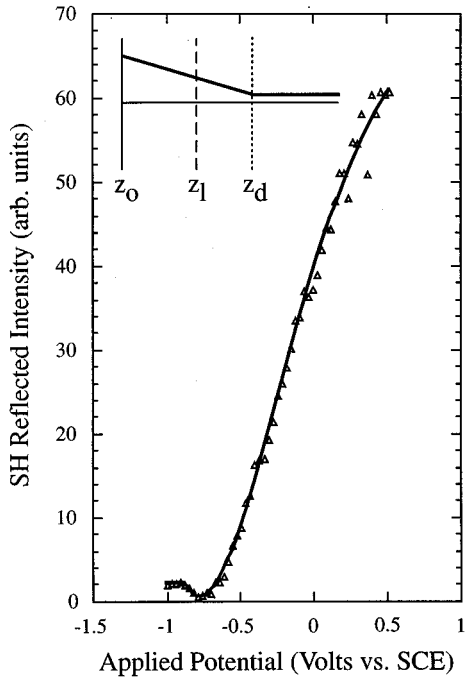

FIG. 8. Results of a curve fit analysis (solid line) of the fixed photon energy, moderate dc field (<388 kV/cm) results of scan *C* in Fig. 6. The triangles are the actual data. The inset shows a schematic of the depletion region with a width (z_d) of 0.05 μm at 301 kV/cm and an attenuation length (z_l) of 0.033 μm for the SH photon energy of the scan (3.43 eV).

VI. CONCLUSION

Field-induced SH from GaN has been observed to enhance the response of the intrinsic second-order susceptibility when the dc field in the GaN sample is on the order of 10^5 V/cm. The sharp spectral response at the direct fundamental band edge indicated the potential of the EFISH technique for spectroscopic analysis of critical points in the JDOS of semiconductors. The localized nature and field-induced broadening of the EFISH response was similar to the

optical resonance observed in linear ER measurements near the E_0 critical point in the JDOS. However, the field-induced EFISH response was considerably larger than the SH flatband response and did not display the Franz-Keldysh oscillations above the band edge that are characteristic of the linear ER measurements.

In addition to the spectral information, SH measurements performed at a fixed frequency and variable dc field determined the value of $\chi^{(3)}_{zzzz}(-2\omega;\omega,\omega,0)$ in the band-edge region to be 5.3×10^{-19} m^2/V^2. Using a bond-charge model to estimate the magnitude of other tensor elements shows that the magnitude of $\chi^{(3)}_{xxxx}(-2\omega;\omega,\omega,0)$ and $\chi^{(3)}_{zzzz}(-2\omega;\omega,\omega,0)$ are 3 and 3.5 times larger than $\chi^{(3)}_{zyyz}(-2\omega;\omega,\omega,0)$, respectively.[47] As such, the EFISH response can be enhanced with an optical excitation scheme that efficiently couples into these diagonal components of the susceptibility. Future EFISH measurements of GaN include an examination of other higher-energy critical points so as to determine the degree of resonant enhancement relative to the fundamental edge.

APPENDIX

In order to calculate the effects of a dc field on the SH response from an intrinsic nonlinear film, one must first solve the linear wave equation for optical fields at 2ω:

$$\nabla^2\vec{E}(z,2\omega)-\frac{\vec{\varepsilon}(2\omega)\omega^2}{c^2}\vec{E}(z,2\omega)=\frac{4\pi\vec{P}^{\rm nl}(z,2\omega)\omega^2}{c^2}, \tag{A1}$$

where $\vec{E}(z,2\omega)$ is the SH field, $\vec{P}^{\rm nl}(z,2\omega)$ is the induced nonlinear polarization, and $\vec{\varepsilon}(2\omega)$ is the unperturbed dielectric function. In deriving expressions for the 2ω reflection coefficient from the electrified electrolyte/GaN interface, field-induced variations in the dielectric function were ignored since the linear ER measurements (as shown in Fig. 5) determined these values to be on the order of 10^{-2}–10^{-3} for dc surface fields up to 10^5 V/cm. This degree of index variation was calculated to produce changes in the SH intensity on the order of 10^{-2} relative to the flatband spectrum, which was orders of magnitude weaker than the $>100\%$ signal variations observed in the SH experimental measurements.

In solving Eq. (A1) in the depletion layer, the primary issue is in properly accounting for the linear variation of the field-dependent nonlinear polarization with distance into the space-charge region [see Eq. (3b)]. In utilizing a reasonable approximation for the dc-field variation *and* deriving tractable solutions for the reflection coefficient, the depletion layer was divided into N individual layers, each of which contained a uniform static field. The region beyond the depletion layer was considered semi-infinite with the nonlinear susceptibility characterized by the intrinsic $\chi^{(2)}_{zyy}(-2\omega;\omega,\omega)$. Applying boundary conditions to the Maxwell's equations at each interface of the N-slice multilayer composite, the following equation was derived for the reflected signal at 2ω:

$$E_r(2\omega)=\left\{E_f(2\omega)\left(\frac{f_2-f_1}{f_2}\right)-\frac{f_3}{f_2}+4\pi f_4\right\}\frac{n_f(2\omega)}{n_r(2\omega)}. \tag{A2}$$

In Eq. (A2), the expression for $E_f(2\omega)$ is given by

$$E_f(2\omega)=\frac{-[2\pi f_2 D(2\omega)+f_3]}{f_1}, \tag{A3}$$

where

$$f_1=\frac{\cos\theta_f(2\omega)n_r(2\omega)+\cos\theta_r(2\omega)n_f(2\omega)}{\cos\theta_r(2\omega)n_r(2\omega)}, \tag{A4a}$$

$$f_2=\frac{\cos\theta_f(2\omega)n_r(2\omega)-\cos\theta_r(2\omega)n_f(2\omega)}{\cos\theta_r(2\omega)n_r(2\omega)}, \tag{A4b}$$

$$f_3=\frac{Q_0 n_r(2\omega)+R_{\cos}\theta_r(2\omega)}{\cos\theta_r(2\omega)n_r(2\omega)}, \tag{A4c}$$

$$f_4=\frac{R_0}{n_f(2\omega)}, \tag{A4d}$$

and

$$Q_0=-\frac{P_z^{\rm nl}(z=0)^{\cos}\theta_f(\omega)^{\sin}\theta_f(\omega)n_f^2(\omega)}{[n_f^2(\omega)-n_f^2(2\omega)]n_f^2(2\omega)}, \tag{A5a}$$

$$R_0=-\frac{n_f(\omega)P_z^{\rm nl}(z=0)^{\sin}\theta_f(\omega)}{n_f^2(\omega)-n_f^2(2\omega)}. \tag{A5b}$$

Also in these expressions,

$$D(2\omega)=\sum_{j=1}^{N} q_j\exp[i\phi(j-1)], \tag{A6}$$

where

$$q_j=\exp(i\phi)\left\{\frac{T_j-Q_{j+1}}{\cos\theta_f(2\omega)}+\frac{R_{j+1}-S_j}{n_f(2\omega)}\right\}, \tag{A7a}$$

$$Q_j=-\frac{P_z^{\rm nl}(z_j)^{\cos}\theta_f(\omega)^{\sin}\theta_f(\omega)n_f^2(\omega)}{[n_f^2(\omega)-n_f^2(2\omega)]n_f^2(2\omega)}, \tag{A7b}$$

$$T_j=Q_j(z_j+\Delta), \tag{A7c}$$

$$R_j=-\frac{n_f(\omega)P_z^{\rm nl}(z_j)\sin\theta_f(\omega)}{n_t^2(\omega)-n_t^2(2\omega)}, \tag{A7d}$$

$$S_j=R_j(z_j+\Delta). \tag{A7e}$$

In Eqs. (A6a)–(A7e), z_i, Δ, and ϕ are

$$z_j=j\frac{z_d}{N}, \tag{A8a}$$

$$\Delta=\frac{z_d}{N}, \tag{A8b}$$

$$\phi=\frac{2\pi^{\cos}\theta_f^{2\omega}n_f(2\omega)\Delta}{\lambda_{\rm SH}}, \tag{A8c}$$

where z_d is the width of the depletion layer. In these expres-

sions, Δ is the width of each individual slice, N is the number of slices, and λ_{SH} is the wavelength of the SH light. In the depleted region, the values for $P^{nl}(z)$ are determined from Eqs. (3b) at the appropriate dc-field value. In all expressions in the Appendix, the angle of transmission in the film (θ_f), reflection from the film (θ_r), refractive index in the GaN film[45,46] (n_f), and refractive index (n_r) in the solution are evaluated at 2ω unless otherwise noted. The term ϕ is equal to the phase shift in each slice of the depletion layer. In the summation in Eq. (A6), the $j=N$ component represents the nonlinearity in the undepleted region where the dc field is zero.

*Author to whom correspondence should be sent.

[1] B. O. Seraphin, in *Proceedings of the Seventh International Conference on the Physics of Semiconductors*, edited by M. Hulin (Dunod, Paris, 1964), p. 165.

[2] J. Callaway, Phys. Rev. **130**, 549 (1963).

[3] D. E. Aspnes, Phys. Rev. **153**, 972 (1966).

[4] Y. Hamakawa, F. A. Germano, and P. Handler, Phys. Rev. **167**, 703 (1968).

[5] B. O. Seraphin and N. Bottka, Phys. Rev. **139**, 560 (1965).

[6] D. E. Aspnes and J. E. Rowe, Phys. Rev. B **5**, 4022 (1972).

[7] D. E. Aspnes and A. A. Studna, Phys. Rev. B **7**, 4605 (1973).

[8] D. E. Aspnes, Surf. Sci. **37**, 418 (1973).

[9] C. H. Lee, R. K. Chang, and N. Bloembergen, Phys. Rev. Lett. **18**, 167 (1967).

[10] B. F. Levine and C. G. Bethea, J. Chem. Phys. **65**, 2429 (1976).

[11] K. D. Singer and A. F. Garito, J. Chem. Phys. **75**, 3572 (1981).

[12] Y. R. Shen, *Principles of Nonlinear Optics*, 1st ed. (Wiley, New York, 1984), Chap. 7.

[13] *Nonlinear Optical Properties of Organic Molecules and Crystals*, edited by D. S. Chemla and J. Zyss (Academic, New York, 1987).

[14] J. R. Helfin, Y. M. Cai, and A. F. Garito, J. Opt. Soc. Am. B **8**, 2132 (1991).

[15] H. Kishida, T. Hasegawa, Y. Iwasa, T. Koda, Y. Tokura, H. Tachibana, M. Matsumoto, S. Wada, T. T. Lay, and H. Tashiro, Phys. Rev. B **50**, 7786 (1994).

[16] L. Tsang, S.-L. Chuang, and S. M. Lee, Phys. Rev. B **41**, 5942 (1990).

[17] L. Tsang and S.-L. Chuang, Phys. Rev. B **42**, 5229 (1990).

[18] L. Tsang and S.-L. Chuang, Appl. Phys. Lett. **60**, 2543 (1992).

[19] O. A. Aktsipetrov, I. M. Baranova, L. V. Grigor'eva, K. N. Evtyukhov, E. D. Mishina, T. V. Murzina, and I. V. Chernyi, Kvant. Elektron. (Moscow) **18**, 943 (1991) [Sov. J. Quantum Electron. **21**, 854 (1991)].

[20] J. Qi, M. S. Yeganeh, I. Koltover, A. G. Yodh, and W. M. Theis, Phys. Rev. Lett. **71**, 633 (1993).

[21] J. M. Lantz and R. M. Corn, J. Phys. Chem. **98**, 4899 (1994).

[22] O. A. Aktsipetrov, A. A. Fedyanin, V. N. Golovkina, and T. V. Murzina, Opt. Lett. **19**, 1450 (1994).

[23] J. Miragliotta, W. A. Bryden, T. J. Kistenmacher, and D. K. Wickenden, in *Diamond, SiC and Nitride Wide Bandgap Semiconductors*, edited by C. H. Carter, Jr., G. Gildenblat, S. Nakamura, and R. J. Nemanich, MRS Symposia Proceedings No. 339 (Materials Research Society, Pittsburgh, 1994), p. 465.

[24] D. K. Wickenden, T. J. Kistenmacher, W. A. Bryden, J. S. Morgan, and A. Estes-Wickenden, in *Heteroepitaxy of Dissimilar Materials*, edited by R. F. C. Farrow, J. P. Harbison, P. S. Peercy, and A. Zangwill, MRS Symposia Proceedings No. 221 (Materials Research Society, Pittsburgh, 1991), p. 167.

[25] P. Blood, Semicond. Sci. Technol. **1**, 7 (1986).

[26] J. Schefold, J. Electrochem. Soc. **139**, 2862 (1992).

[27] J. Miragliotta and D. K. Wickenden, Phys. Rev. B **50**, 14 960 (1994).

[28] L. Szaro, Surf. Sci. **137**, 311 (1983).

[29] R. A. Batchelor, A. C. Brown, and A. Hamnett, Phys. Rev. B **41**, 1401 (1990).

[30] R. A. Batchelor, A. Hamnett, R. Peat, and L. M. Peter, J. Appl. Phys. **70**, 266 (1991).

[31] R. A. Batchelor and A. Hamnett, J. Appl. Phys. **71**, 1376 (1992).

[32] R. Reineke and R. Memming, J. Phys. Chem. **96**, 1310 (1992).

[33] W. Schottky, Z. Phys. **118**, 539 (1942).

[34] J. Schefold and M. Vetter, J. Electrochem. Soc. **141**, 2040 (1994).

[35] A. Nussbaum, in *Contacts, Junctions, Transport*, edited by R. Willardson and A. C. Beer, Semiconductor and Semimetals Vol. 15 (Academic, New York, 1981), p. 39.

[36] N. Bloembergen and P. S. Pershan, Phys. Rev. **128**, 606 (1962).

[37] R. Boyd, *Nonlinear Optics* (Academic, New York, 1992), Chap. 1.

[38] N. Bloembergen, *Nonlinear Optics* (Benjamin-Cummings, New York, 1965), Chap. 4.

[39] D. J. Moss, J. E. Sipe, and H. M. van Driel, Phys. Rev. B **36**, 9708 (1987).

[40] E. Ghahramani, D. J. Moss, and J. E. Sipe, Phys. Rev. B **43**, 9700 (1991).

[41] E. Ghahramani, D. J. Moss, and J. E. Sipe, Phys. Rev. B **43**, 8990 (1991).

[42] J. E. Sipe and E. Ghahramani, Phys. Rev. B **48**, 11 705 (1993).

[43] S. Logothetidis, J. Petalas, M. Cardona, and T. D. Moustakas, Phys. Rev. B **50**, 18 017 (1994).

[44] D. J. Moss, E. Ghahramani, J. Sipe, and H. M. van Driel, Phys. Rev. B **41**, 1542 (1990).

[45] H. Amano, N. Watanabe, N. Koide, and I. Akasaki, Jpn, J. Appl. Phys. **32**, L1000 (1993).

[46] Ejder, Phys. Status Solidi A **6**, 442 (1971).

[47] B. F. Levine, Phys. Rev. B **7**, 2600 (1973).

[48] *Semiconductors Physics of Group IV Elements and III-V Compounds*, edited by O. Madelung, Landölt-Bornstein, New Series, Group III, Vol. 17, Pt. a (Springer, Berlin, 1991), p. 89.

[49] B. B. Kosicki, R. J. Powell, and J. E. Burgiel, Phys. Rev. Lett. **24**, 1421 (1970).